Nucleation-limited amorphization of GaAs at elevated temperatures

R. A. Brown*
School of Physics, University of Melbourne, Parkville 3052, Australia

J. S. Williams
Research School of Physical Sciences and Engineering, Australian National University, Canberra, ACT 0200, Australia
(Received 2 December 1996)

By a detailed correlation of damage profiles from Rutherford backscattering and channeling with cross-sectional transmission electron microscopy images, we have identified an intriguing nucleation-limited amorphization regime in GaAs irradiated with ions at elevated temperatures. When the rate of dynamic annealing during irradiation exceeds the damage production rate, amorphization can take place at depths significantly different from the maximum in the energy deposition density. This process results from the incomplete annihilation of mobile irradiation-induced defects and occurs either at the surface or at a dislocation band, formed by the agglomeration of interstitials. Once formed, such amorphous layers grow by a layer-by-layer process. [S0163-1829(97)00520-1]

Early observations of damage accumulation and amorphization in GaAs identified strong dynamic recovery of implantation-induced defects during irradiation. The amount and nature of residual disorder was found to exhibit strong temperature and ion flux dependences close to room temperature.[1] When the observed dynamic annealing rate is considerably lower than the defect production rate (typically, at temperatures $<50\ ^\circ$C), early models of the amorphization process seem to be appropriate. Broadly speaking, these models can be divided into two types: heterogeneous and homogeneous. The heterogeneous models postulate that the production of amorphous layers occurs via the accumulation of amorphous zones.[2] Conversely, homogeneous models view amorphization as resulting from the accumulation of point defects, producing the amorphous phase by collapse of the lattice when the free energy of the defective crystal exceeds that of the amorphous phase.[3]

Recently, when the rate of dynamic annealing is close to, or exceeds damage production, very sharp temperature and ion flux dependences have been observed. For example, when irradiating at elevated temperatures of typically $\approx 50-70\ ^\circ$C, variations of only a few degrees can give dramatically different damage structures, ranging from thick amorphous layers to barely visible disorder.[4] In such cases, where irradiation-induced defects are quite mobile, damage accumulation and the pathway to amorphization might be expected to depart from early models which do not consider long-range defect migration, the role of secondary (extended) defects formed by point defect agglomeration, and defect annealing and trapping processes which occur long after ($\sim$seconds) the ion cascade has quenched.

In this paper, we report on a detailed microstructural investigation of amorphous phase production at elevated temperatures in GaAs where the rate of dynamic annealing balances or exceeds the damage production rate. Strong evidence for nucleation-limited amorphization is obtained.

Pieces of single-crystal, semi-insulating, (100) GaAs were mounted onto a temperature-controlled nickel target block with conducting silver paste. Ions of 95 keV, $^{28}Si^-$ were produced by a 1.7 MV NEC tandem ion implanter at a constant flux of 4.8×10^{13} Si cm^{-2} s^{-1}. After implantation, samples were analyzed by Rutherford backscattering and channeling (RBS) with 2-MeV He ions, backscattered into detectors at 100° and $\simeq$170° to the incident-beam direction. Selected samples were also analyzed by cross-sectional transmission electron microscopy (XTEM) to examine the damage microstructure.

Following elevated temperature bombardment, the distribution of residual damage in GaAs can depart quite substantially from that expected from the nuclear energy deposition distribution. This is illustrated in Fig. 1(a), which shows a RBS depth profile of damage resulting from 95 keV, 1×10^{16} Si cm^{-2} bombardment at 88 °C. Also shown by the dashed curve is the nuclear energy deposition obtained from TRIM.[5] Clearly, the damage accumulates preferentially at the surface (surface peak approaching the random level) and also beyond the peak of the energy deposition distribution (as indicated by the high dechanneling rate between depths of 30 and 90 nm). Figure 1(b) illustrates the microstructure of this bimodal damage distribution, using XTEM. A thin ($\simeq$10 nm) amorphous layer is formed at the surface, together with a deeper band consisting mainly of dislocations, extending from a depth of 30–40 nm down to 90–100 nm. This dislocation band gives rise to the rapidly increasing RBS yield at about 30–90 nm in Fig. 1(a). Beyond this depth, small spots of dark contrast extend to depths of $\simeq$120 nm. Between the surface amorphous layer and the dislocation band is a region of crystal, practically free of visible defects.

The residual microstructure illustrated in Fig. 1 points to strong migration, annihilation, and agglomeration of irradiation-induced defects. The amorphous layer formed at the surface presumably originates from the trapping of defects (of vacancy and/or interstitial type). Such defect accumulation may ultimately result in the ''collapse'' of this defective crystalline region into an amorphous phase when its free energy exceeds that of amorphous GaAs. Thus, amorphous phase nucleation at the surface can occur even under conditions where dynamic annealing just below the surface dominates defect production. Indeed, the surface may act as

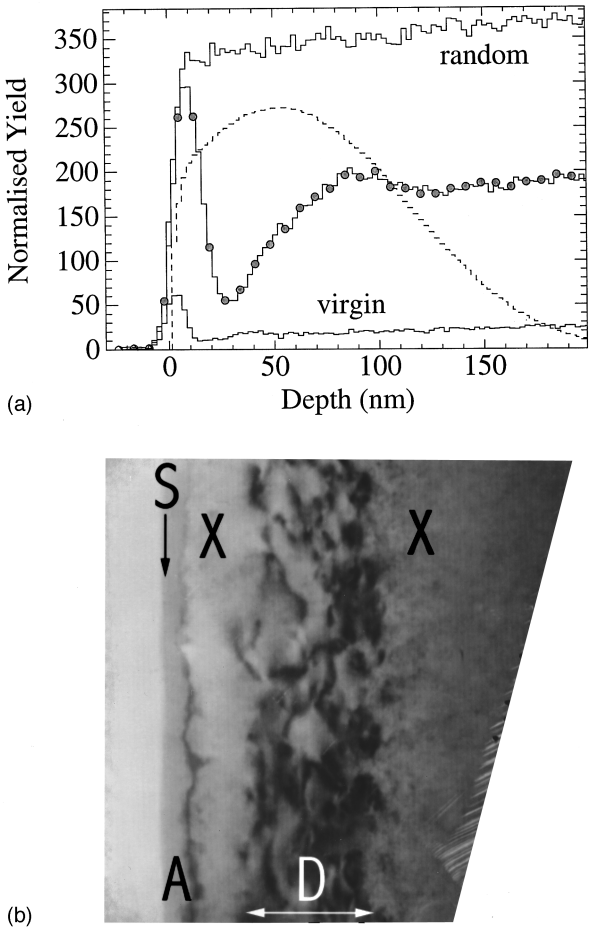

FIG. 1. The damage distribution in (100) GaAs implanted with 95 keV, 1×10^{16} Si cm^{-2} at 88 °C (flux 4.8×10^{13} Si cm^{-2} s^{-1}) as measured by (a) RBS depth profiling and (b) cross-sectional TEM microscopy. The dashed curve in (a) indicates the nuclear energy deposition distribution with a peak at $\simeq$50 nm. Depth profiles from unirradiated (''virgin'') and nonaligned (''random'') GaAs are shown for comparison. The XTEM image in (b) shows an amorphous layer (A) at the surface (S), a region of good crystal (X), and a deeper band of dislocations (D). The depth scale of the XTEM micrograph is given by the RBS profile.

a gettering region for irradiation-induced defects, leaving the region below the surface substantially free of visible defects, consistent with our observations. Once the amorphous phase has nucleated, it grows, through defect accumulation, into the underlying crystalline regions with further irradiation, ultimately consuming the dislocation band. Also, a deep band of dislocations forms near and beyond the projected range of implanted ions to reduce the compressive strain resulting from the large concentration of excess atoms at this depth. These excess atoms originate from both the implanted ions themselves, and interstitials from the collision cascade. This latter effect arises from the displacement in depth of vacancies and interstitials generated within the collision cascade. The excess of interstitials at greater depths may be initially estimated by calculating the net interstitial population, i.e., by subtracting the vacancy depth profile from the interstitial profile.[6–8] There is a consequential vacancy excess closer to the surface following the quenching of the collision cascade, but the ultimate interstitial and vacancy distributions may be

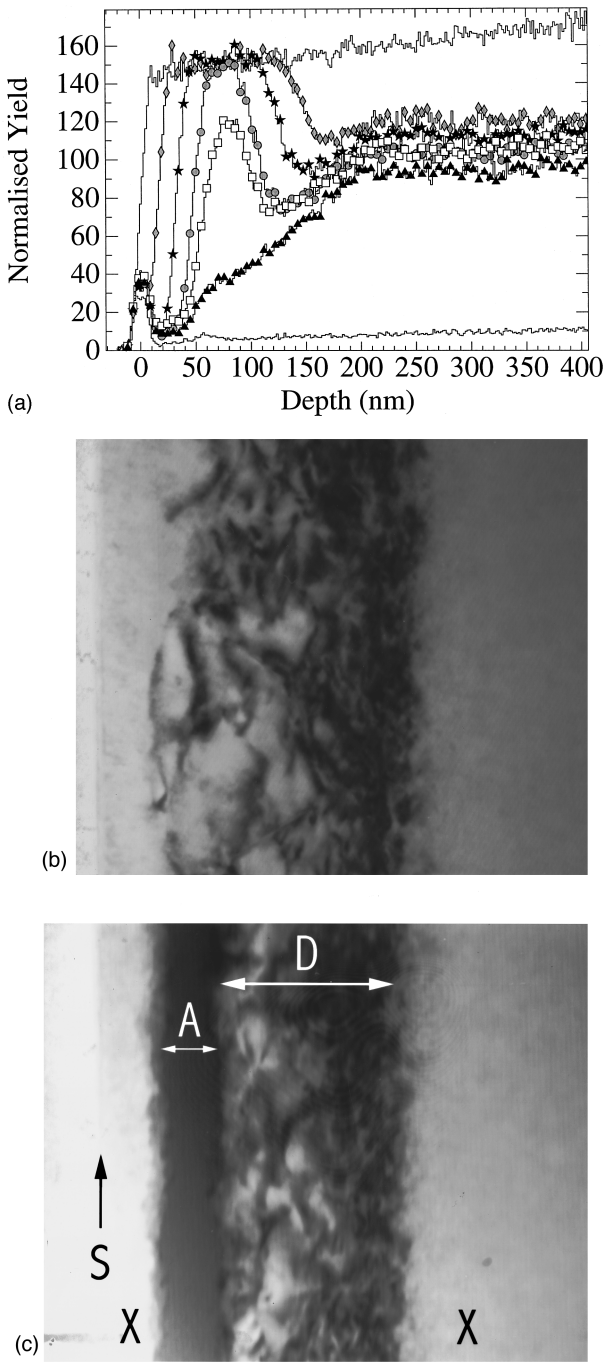

FIG. 2. (a) RBS depth profiles illustrating the accumulation of crystal damage in (100) GaAs implanted with 95 keV Si at 110 °C. Fluences are 3.0×10^{16} cm^{-2} (triangles), 3.3×10^{16} cm^{-2} (squares), 3.4×10^{16} cm^{-2} (circles), 3.9×10^{16} cm^{-2} (stars), and 6.0×10^{16} cm^{-2} (diamonds). (b) XTEM image showing the damage resulting from implantation with 95 keV, 2.8×10^{16}Si cm^{-2} at 110 °C. A deep band of dislocations may be seen, extending beyond the depth of maximum energy deposition to $\approx$250 nm. (c) XTEM image showing the damage resulting from implantation of the higher fluence of 3.1×10^{16} Si cm^{-2} at 110 °C. A buried, continuous amorphous layer (A) has nucleated on the buried dislocations (D). The depth of this layer is greater than the depth of maximum energy deposition. The surface is indicated by the arrow S, and good quality crystal is indicated by X.

appreciably altered by defect migration, annihilation, and agglomeration.

A distinctly different amorphization regime is observed for implantation at a mere 25 °C higher. Figure 2(a) shows RBS depth profiles from samples implanted at 110 °C at fluences from 3.0×10^{16} cm^{-2} to 6.0×10^{16} cm^{-2}. Figure 2(b) shows a XTEM image from the sample implanted with the lowest fluence, 3.0×10^{16} cm^{-2}. Similar to the sample implanted at 88 °C, this sample contains a buried band of dislocations. However, at this higher temperature, the dislocation band extends down to a depth of $\simeq$250 nm, compared with a depth of only $\simeq$100 nm at the lower temperature. This presumably relates to the enhanced mobility of excess interstitials. In addition, the amorphous surface layer observed at the lower temperature is completely absent here. Indeed, selected-area diffraction provided no evidence for amorphization at any depth for this fluence, and the TEM observations are consistent with residual damage dominated by complexes and dislocations arising from the coalescence of interstitials. However, at higher ion fluences, a direct scattering peak appears in the RBS depth profiles, and builds up to the random level by a fluence of 3.4×10^{16} cm^{-2}. When corrected for the lower channeled stopping power of 2-MeV He in GaAs along the incident path,[9] the damage peak is centered at $\simeq$90 nm, which is substantially deeper than the peak of the nuclear energy deposition distribution ($\simeq$50 nm) shown in Fig. 1. We note that the buildup of a disorder peak at substantially lower irradiation temperatures occurs at depths which correspond more closely to the peak of the nuclear energy deposition distribution.[4] This presumably reflects the lower mobility of irradiation-induced defects and the formation of secondary defects close to the depth of defect generation.

The reason for the sudden rise of the disorder peak at a fluence of 3×10^{16} cm^{-2} is provided by the data of Fig. 2(c) which shows a typical XTEM image corresponding to the RBS spectrum for the 3.4×10^{16} cm^{-2} case shown in Fig. 2(a). A continuous amorphous layer has formed at the front of the dislocation band. We propose that, under these conditions where the dynamic annealing rate effectively exceeds the damage production rate, amorphization is suppressed until the density of residual defects (at the dislocation band) exceeds a threshold value corresponding to a critical free energy. Dislocations are known to getter mobile defects[10] and impurities[11] in GaAs, thus adding to defect accumulation at the dislocation band. Therefore, dislocations provide suitable nucleation sites for localized collapse to the amorphous phase in cases where the free energy of the defective crystal exceeds that of the amorphous phase. In this situation, we suggest that amorphization is nucleation limited and can initiate at favorable defect gettering sites removed from the peak of the energy deposition distribution.

Once nucleated, the amorphous layer becomes a stable growth site. With increasing fluence, RBS and XTEM show that this layer grows in thickness. Because it grows in a quasi-layer-by-layer fashion, the layer is continuous. This is not the case for layers formed at lower temperatures for the same ion flux, where multiple nucleation sites may exist at secondary defects formed close to the peak of the nuclear deposition distribution. Furthermore, the amorphous layer initially extends more rapidly with increasing fluence towards the surface, which is not surprising in view of the higher concentration of irradiation-induced defects supplied on this side of the amorphous layer.

Previously, amorphous layer growth has been observed at existing *a-c* interfaces[12] and at dislocation bands[13] in Si. For example, layer-by-layer amorphization has been stimulated by MeV ion implantation of preexisting amorphous layers in Si, and this is thought to be attributable to the trapping of mobile divacancies[12] or to the agglomeration of more complex defects at the amorphous-crystalline interface.[14] In GaAs, our data suggests a similar process for the growth of amorphous layers, once nucleated, although it is not possible as yet to identify the specific defects responsible. Compared with Si, the nature of the amorphization process changes dramatically over a very narrow temperature range, in our case from near-normal damage accumulation and amorphization at $<$80 °C, through surface nucleation at $\simeq$90 °C, to nucleation on dislocated material at $\gtrsim$95 °C.

The notion of nucleation-limited amorphization in GaAs has previously been inferred from the anomalous damage buildup in GaAs-AlAs superlattices at 80–90 K.[15] These authors suggested that amorphization was likely to have taken place at regions containing extended defects, and not by the accumulation of point defects. Our results provide direct evidence for such a process under elevated temperature irradiation conditions.

In conclusion, we have demonstrated that the amorphization of GaAs, under ion irradiation conditions where the rate of dynamic annealing exceeds the defect production rate, can occur at depths which are shallower or deeper than the maximum in the nuclear energy deposition distribution. We propose that such amorphization is nucleation limited and initiates in regions where residual defects accumulate (either at the surface or at extrinsic dislocations). Amorphization is favored when the free energy of defective crystalline regions exceeds that of the amorphous phase.

We would like to thank Rob Elliman for assistance with the TEM.

*Present address: Department of Materials Science and Engineering, North Carolina State University, Raleigh, NC 27695-7916.

[1] W. H. Weisenberger, S. T. Picraux, and F. L. Vook, Radiat. Eff. **9**, 121 (1971).
[2] F. Morehead, Jr. and B. L. Crowder, Radiat. Eff. **6**, 27 (1970).
[3] F. L. Vook and H. J. Stein, Radiat. Eff. **2**, 23 (1969).
[4] R. A. Brown and J. S. Williams, J. Appl. Phys. (to be published).
[5] J. P. Biersack and L. G. Haggmark, Nucl. Instrum. Methods **174**, 257 (1980).
[6] K. B. Winterbon, Radiat. Eff. **46**, 181 (1980).
[7] L. A. Christel and J. F. Gibbons, Radiat. Eff. **46**, 181 (1980).
[8] A. M. Mazzone, Phys. Status Solidi A **95**, 149 (1986).
[9] R. A. Brown, Ph.D. thesis, University of Melbourne, 1995.
[10] J. C. Bourgoin, H. J. von Bardeleben, and D. Stiévenard, J. Appl. Phys. **64**, R65 (1988).
[11] I. Yonenaga and K. Sumino, J. Appl. Phys. **65**, 85 (1989).
[12] J. Linnros, R. G. Elliman, and W. L. Brown, J. Mater. Res. **3**, 1208 (1988).

[13] J. S. Williams, H. H. Tan, R. D. Goldberg, R. A. Brown, and C. Jagadish, in *Materials Synthesis and Processing Using Ion Beams*, edited by R. J. Culbertson, O. W. Holland, K. S. Jones, and K. Maex, MRS Symposia Proceedings No. 316 (Materials Research Society, Pittsburgh, 1994), pp. 15–25.

[14] P. J. Schultz, C. Jagadish, M. C. Ridgway, R. G. Elliman, and J. S. Williams, Phys. Rev. B **44**, 9118 (1991).

[15] D. J. Eaglesham, J. M. Poate, D. C. Jacobson, M. Cerullo, L. N. Pfeiffer, and K. West, Appl. Phys. Lett. **58**, 523 (1991).